Carbohydrate Polymers 87 (2012) 1532–1538

Contents lists available at SciVerse ScienceDirect

Carbohydrate Polymers

journal homepage: www.elsevier.com/locate/carbpol

Tailoring carboxymethyl guargum hydrogel with nanosilica for sustained transdermal release of diclofenac sodium

Arindam Giri[a], Totan Ghosh[b], Asit Baran Panda[c], Sagar Pal[d], Abhijit Bandyopdhyay[a,*]

[a] Department of Polymer Science and Technology, University of Calcutta, 92, A.P.C. Road, Calcutta 700009, India
[b] Department of Chemistry, University of Calcutta, 92, A.P.C. Road, Calcutta 700009, India
[c] Disciplines of Inorganic Materials and Catalysis, Central Salt and Marine Chemicals Research Institute (CSMCRI), Bhavnagar 364021, Gujarat, India
[d] Department of Applied Chemistry, Indian School of Mines, Dhanbad 826004, India

ARTICLE INFO

Article history:
Received 22 July 2011
Received in revised form 2 September 2011
Accepted 13 September 2011
Available online 19 September 2011

Keywords:
CMG
Nanosilica
Morphology
Swelling
Sustained release

ABSTRACT

Carboxymethyl guar gum (CMG) was structurally tailored with aqueous-nanosilica sol for controlled transdermal release of diclofenac sodium. Nanosilica was administered in low to moderately high concentration range to synthesize various, novel CMG–silica hybrid nanocomposites. Spectroscopy together with thermogravimetry, morphology, swelling and rheological studies proved that 1 wt% nanosilica content was the best physical formulation. The drug release studies from different hydrogel nanocomposites exhibited slower release than neat CMG. 1 wt% nanosilica loaded hydrogel nanocomposite gave slowest but steady release profile among all other nanocomposites due to its highly viscous nature owing to most compact microstructure.

1. Introduction

Controlled or sustained delivery of various drugs/biomolecules has been the priority research area in medicinal biotechnology since number of years (Adnadjevic, Jovanovic, & Drakulic, 2007; Moskowitz et al., 2010; Srinivas, Sunitha, Babu, & Sadanandam, 2011). It involves multi-disciplinary scientific approach that aim towards human health care and beneficiation (Ali et al., 2007; Lee, Kung, & Lee, 2005; Meenach, Hilt, & Anderson, 2010). Excess drug consumption, which often leads to various toxic side effects, can be reduced by prolonging the release and patient compliance and convenience are thereby improved by maintaining low to moderately high drug concentration in the blood. Over the decades various innovative routes for sustained/controlled drug administration have been reported (Ji et al., 2010; Peng et al., 2010; Siddaramaiah, Kumar, Divya, Mhemavathi, & Manjula, 2006). Out of the several, transdermal route seems to be an excellent technique especially for those drugs having severe side effects on overdose or having shorter half life or are extremely painful during intravenous administration (Lolis, Toosi, Czernik, & Bystryn, 2011; Trachsel et al., 2004). Diclofenac sodium, prescribed for treating rheumatoid arthritis, is an example of such a drug having severe side effects related to gastro-intestinal and renal dysfunctions on prolonged intake (Altman and Barkin, 2009; Banning, 2006; Magnette et al., 2004). It also has a meagre half life of only 2 h which ultimately sets it as an ideal contender for controlled/sustained delivery approach to maintain low drug concentration in the blood. Synthetic/natural biocompatible polymers are widely investigated as controlled release device over the years (Cassano, Trombino, Muzzalupo, Tavano, & Picci, 2009; Lin, Chen, & Luo, 2007; Nugent & Higginbotham, 2007). Natural polymers are edge-ahead in this experimentation due to its more bio-friendly character compared to synthetic variety (He, Cao, & Lee, 2004; Liang et al., 2006; Singh & Pal, 2008). Diclofenac sodium has limited water solubility and its elution could be efficiently controlled if the device shows proportionally higher hydrophobic character (Giri, Bhowmick, Pal, & Bandyopadhyay, 2011). But, at the same time, hydrophilicity and viscosity has to be enhanced to encapsulate drug molecules and so, the device needs to be engineered critically. Natural polymers, though preferred for such application, are all highly hydrophilic and mechanically very weak (Diez-Pascual et al., 2010; Spitalsky, Tasis, Papagelis, & Galiotis, 2010; Tjong, 2006). We, in this study, have tried to alleviate these issues by ex situ nanosilica administration into a semi-synthetic polysaccharide matrix, carboxymethyl guar gum (CMG), targeted as transdermal device for delivering diclofenac sodium. CMG is low cost, chemically modified native guar gum having degree of substitution 0.6 (Pal, 2009). It has greater water solubility and viscosity than guar gum. Nanosilica is expected to cater high mechanical strength and low swelling

* Corresponding author. Tel.: +91 033 235013976996/6387/8386x288.
E-mail addresses: abpoly@caluniv.ac.in, abhijitbandyopadhyay@yahoo.co.in (A. Bandyopdhyay).

0144-8617/$ – see front matter © 2011 Elsevier Ltd. All rights reserved.
doi:10.1016/j.carbpol.2011.09.050

property (Bandyopadhyay, De Sarkar, & Bhowmick, 2005a, 2005b; Bandyopadhyay, De Sarkar, & Bhowmick, 2006) which may facilitate controlled/sustained delivery of diclofenac sodium. Aqueous nanosilica sol has been added to aqueous CMG within low to moderately high concentration regime to optimize physico-rheologically the best composition for transdermal delivery application.

2. Experimental

2.1. Materials

Carboxymethyl guar gum (CMG, DS 0.6) stabilized with excess sodium hydroxide at pH 11.0 was kindly supplied by Hindustan Gum and Chemicals Ltd., Haryana, India. Aqueous nanosilica sol (25% silica content), stabilized at pH 9.0 was generously supplied by Bee Chem, Kanpur, India. Sodium lauryl sulphate (SLS, 98% pure) of standard laboratory grade was purchased from Loba Chem., Mumbai, India. Diclofenac sodium, a pain reliever drug was a gift sample received from Ranbaxy Int. Gurgaon, Haryana, India.

2.2. Sample preparation

Nanosilica was ultrasonically dispersed in 5% (w/v) aqueous CMG sol in different weight concentrations (with respect to CMG) like 0.5, 1, 3 and 5 at room temperature in presence of 1 wt% SLS (sodium lauryl sulphate) with respect to nanosilica, to form the hybrid hydrogels. SLS was used as silica dispersing agent. pH of the nanocomposites was adjusted to 7.0 by adding appropriate amount of *N*/10 HCl (AR). 1 mg diclofenac sodium was ultrasonically mixed thereafter in each hydrogel including neat CMG to produce drug encapsulated hydrogels for physico-rheological and release analysis. Designation and detailed composition of the samples are listed in Table 1.

2.3. Characterization

Spectroscopic characterization of hybrid nanocomposites was done through Fourier transform infrared (FTIR) spectrophotometer, JASCO FTIR, within the spectral range of 400–4000 cm^{-1} and resolution 4 cm^{-1} and, solid state ^{13}C and ^{29}Si nuclear magnetic resonance (NMR) spectrophotometer (Bruker, 500 MHz) under ambient condition. Thermal stability from room temperature (27 °C) to 600 °C was tested in a Thermogravimetric analyzer (Perkin Elmer), using a heating rate of 10 °C/min under nitrogen. Morphological study of hybrid nanocomposites was accomplished in an Atomic Force Microscope from Digital Instruments (Nanoscope III) under trapping mode. Rheological measurements were carried out in a HAAKE Viscotester 550, Thermo Scientific, Germany within the shear rate range of near zero to 400 S^{-1} under ambient condition. Transdermal drug release experiment was carried out in Franz diffusion cell. Detail description of the procedure related to release analysis has been described in our earlier publication (Bhunia, Goswami, Chattopadhyay, & Bandyopadhyay, 2011). Eluted concentration of diclofenac sodium during experimentation was spectrophotometrically analyzed at 276 nm after consulting a standard calibration curve. Each experiment was repeated thrice and standard deviation was calculated to check accuracy level of each data.

3. Results and discussion

3.1. FTIR spectroscopic analysis

FTIR spectra of neat CMG and different CMG–nanosilica hybrid hydrogels are displayed in Fig. 1a. Each spectrum shown in the figure is designated to address ex situ nanosilica contents in each of

Table 1
Sample composition, rheological parameters and drug release kinetics of CMG and its hybrid nanocomposites.

Hydrogel designation	CMG (wt%)	Nanosilica (%)	Sodium lauryl sulphate (SLS) (wt%)	*n*	ln *K*	SD	r^2	Zero-order r^2	First-order r^2	Higuchi r^2	Korsmeyer–Peppas *m*
CMG	5.0	0.0	1	−2.63500	2.63500	0.01623	−0.92695	0.93622	0.97314	0.98965	0.56730
$CMG_{0.5}$	5.0	0.5	1	−2.71288	2.71288	0.01149	−0.92275	0.98945	0.99587	0.98859	0.72353
$CMG_{1.0}$	5.0	1.0	1	−2.83533	2.83533	0.01932	−0.90864	0.99254	0.99716	0.98675	0.78348
$CMG_{3.0}$	5.0	3.0	1	−2.67113	2.67113	0.01277	−0.91222	0.97614	0.98976	0.99411	0.65808
$CMG_{5.0}$	5.0	5.0	1	−2.61419	2.61419	0.01571	−0.09026	0.95204	0.97578	0.99274	0.60812

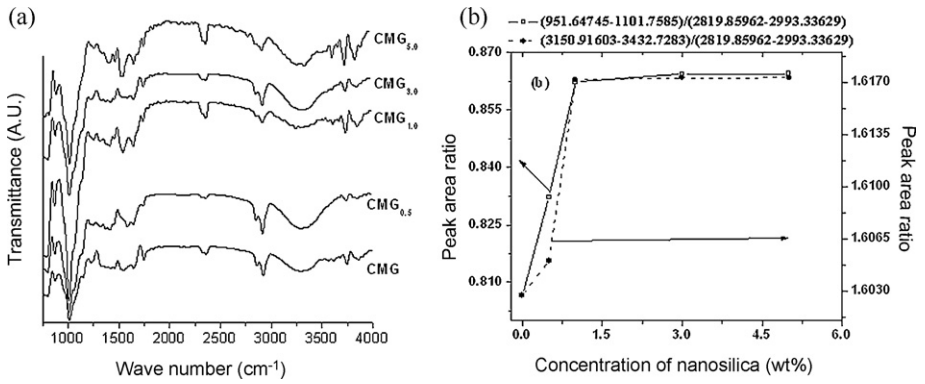

Fig. 1. (a) Normalized FTIR spectra of neat CMG and its hybrid nanocomposites and (b) peak area ratio vs. various nanosilica contents in hybrid hydrogels.

these nanocomposites. Neat CMG shows its characteristic peaks at 3297, 1744 and 1135 cm^{-1} on account of –OH, C=O and C–O bond vibrations. The broad band at 3297 cm^{-1} also includes the contribution from absorbed moisture apart from –OH groups of the CMG itself. In hybrid nanocomposites, transmittances related to O–H, Si–O–Si and C=O bond/group vibrations may be scanned to understand microstructural changes. Fig. 1b shows variation in two of these transmission peak areas (O–H and Si–O–Si) after normalization against hydrocarbon peak transmissions (peaks near 2900 cm^{-1}) for different ex situ nanosilica hybrids. Band area corresponding to O–H bond vibration in neat CMG has slightly increased up to 1 wt% nanosilica content and then has decreased marginally for rest of the two compositions. Inflated band area indicates presence of more O–H bonds which actually comes from uncondensed silanol (Si–O–H) groups of ex situ nanosilica sol. But the peak area does not increase beyond $CMG_{1.0}$ despite more silica content. It is possibly due to selfcondensation tendency of silica nanoparticles utilizing its surface silanol groups. The pronounced band centered around 1010 cm^{-1} in neat CMG shows a clear hump ranging between 1060 and 1090 cm^{-1} in its nanocomposites (Fig. 1a). It comes from Si–O–Si asymmetric stretch of silica nanoparticles present in the hybrid hydrogels. At higher silica loading i.e. in $CMG_{3.0}$ and $CMG_{5.0}$ this hump appears close to 1090 cm^{-1} for predominant Si–O–Si ring structure in silica phase whereas at low silica content i.e. in $CMG_{0.5}$ and $CMG_{1.0}$, it appears around 1060 cm^{-1} indicating more linear silica configuration. The entire band area of this region has increased up to $CMG_{1.0}$ due to increasing nanosilica content; thereafter it remains constant in $CMG_{3.0}$ and $CMG_{5.0}$ (Fig. 1b). At higher silica loading hydrogels may become more heterogeneous due to silica aggregation (Giri et al., 2011), leading to non-uniform distribution and are thus not detected. Peak transmittance at 1744 cm^{-1} in neat CMG, assigned to C=O stretches, has downwardly shifted to 1725 cm^{-1} accounting hydrogen bonded interaction between nanosilica and CMG. Similarly hydrocarbon stretches at 2930 cm^{-1} in neat CMG has lowered to 2918 cm^{-1} owing to adsorption of CMG over silica nanoparticles in the hybrid hydrogels.

3.2. ^{13}C and ^{29}Si NMR spectroscopic analysis

^{13}C NMR spectra of neat CMG and its hybrid nanocomposites are compared in Fig. 2a. Neat CMG (Fig. 2a) reveals five distinct peaks: (i) at δ = 177 ppm for carboxyl carbon of COOH moiety, (ii) at δ = 107.4 ppm for the anomeric carbon atom, (iii) at δ = 80.6 ppm for all the carbon atoms in the six membered ring attached to O–H group except annomeric carbon atom, (iv) at δ = 68.0 ppm is for carbon atoms of $-CH_2-O-CH_2-COOH$ moiety and finally (v) peak at δ = 77.0 ppm for the carbon atom in chemically inserted $-O-CH_2$ portion of CMG.

These δ values of both $CMG_{1.0}$ (Fig. 2b) and $CMG_{3.0}$ (Fig. 2c) are shifted towards down field as compared to neat CMG. This is primarily due to attractive interaction between nanosilica and CMG mediated through hydrogen bonding. Additionally, it also indicates adsorption of more CMG units over nanosilica particles in these hybrids. For each NMR peak $CMG_{1.0}$ has recorded slightly greater downward shift as nanosilica creates better interaction with CMG at this concentration.

As an additional evidence, ^{29}Si NMR spectrum of $CMG_{1.0}$ in Fig. 2d shows the presence of two distinct signals at −91, −98 ppm and the prime signal at −108 ppm corresponding to $(-O-)_2$ $Si(OH)_2$ with two OH groups (Q^2), $(-O-)_3$ Si(OH) with one OH group (Q^3) and $(-O-)_4$ Si with no OH group (Q^4) as prime silica configuration which means, the free silanol groups in most of the silica nanoparticles are actively engaged in hydrogen bonding with CMG segments in the nanocomposite.

3.3. Thermogravimetric analysis

TG and DTG profiles of neat CMG and its nanocomposites are compared in Fig. 3a and b. Largely, there are two major weight losses in neat CMG – the first one at 275 °C due to removal of bound moisture and degradation of the branch units and the second one, occurring within the range of 430–480 °C, due to main chain degradation. Advent of nanosilica into CMG has brought about some noticeable changes in the degradation pattern. In the first phase, the extent of degradation has been prominently delayed primarily due to low bound moisture levels and CMG–silica adhesive interaction. In the second phase the degradation loss is more prominent in the nanocomposites as compared to neat CMG but it is considered to be less significant from practical standpoint since it occurs much above the ambient. Thus it can be presumed that silica nanoparticles has slightly improved the thermal stability of CMG at the initial phase of degradation but in the later stage has accelerated the same.

3.4. Visual transparency and Atomic Force Microscopic studies

Visual transparency has been tested on different nanosilica containing hybrid hydrogels. The thin hydrogel films (thickness 0.25 mm) were placed on arbitrary letters and were photographed from the top using a digital camera (Sony 10.1 mega pixels Fig. 4a). Nanocomposites become transparent to opaque with increasing concentration of nanosilica. At low concentration silica particles are primarily at nanolevel i.e. they do not scatter light and offers high transparency. At high concentration these silica nanoparticles tend to aggregate and form bigger domains which scatter light and make the sample opaque.

Tapping mode AFM images of two representative dry films of hybrid nanocomposites were scanned for more morphological

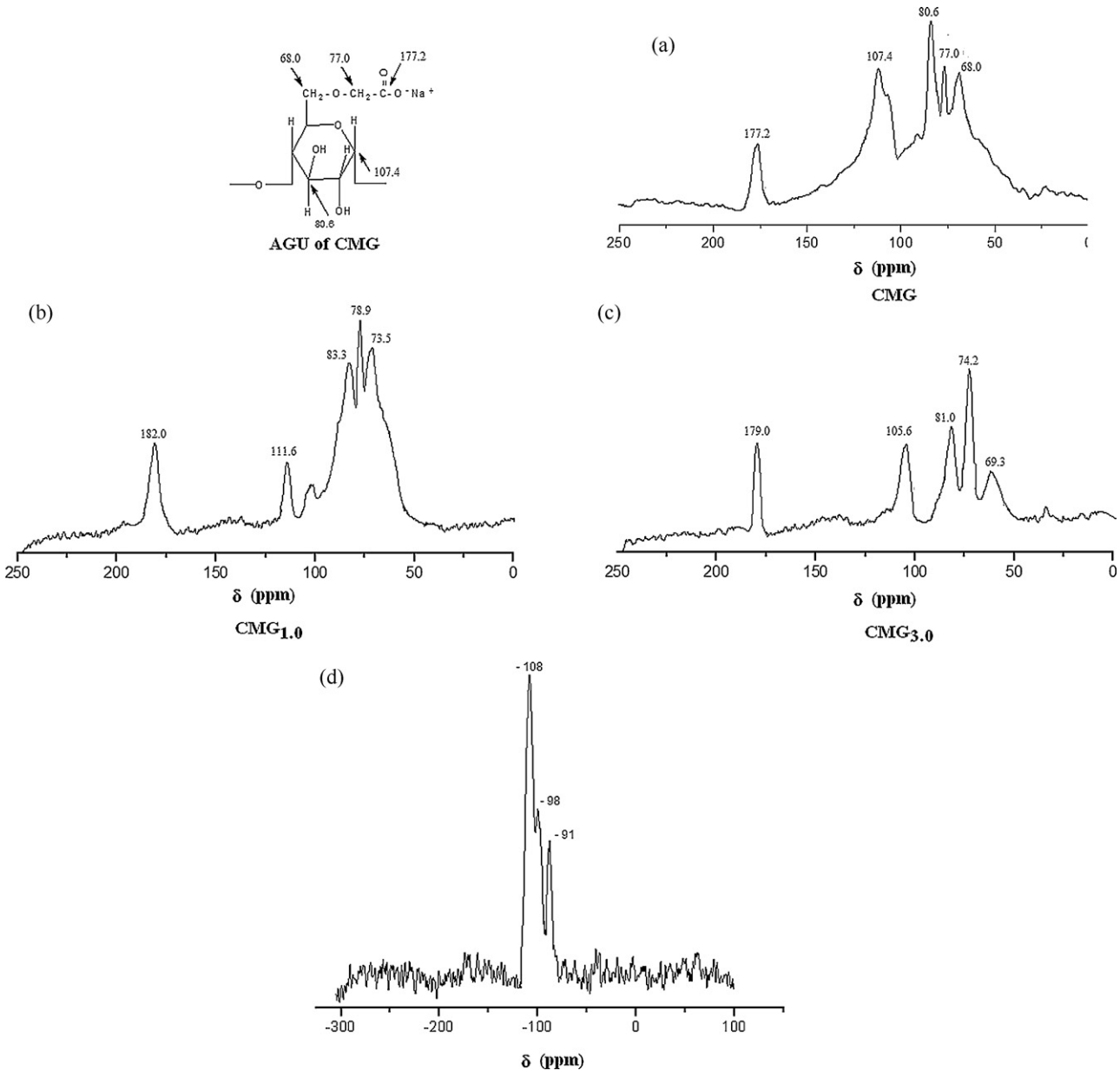

Fig. 2. Solid state ^{13}C NMR spectra of (a) neat CMG, (b) $CMG_{1.0}$ and (c) $CMG_{3.0}$ and (d) ^{29}Si NMR spectrum of $CMG_{1.0}$ hybrid nanocomposite.

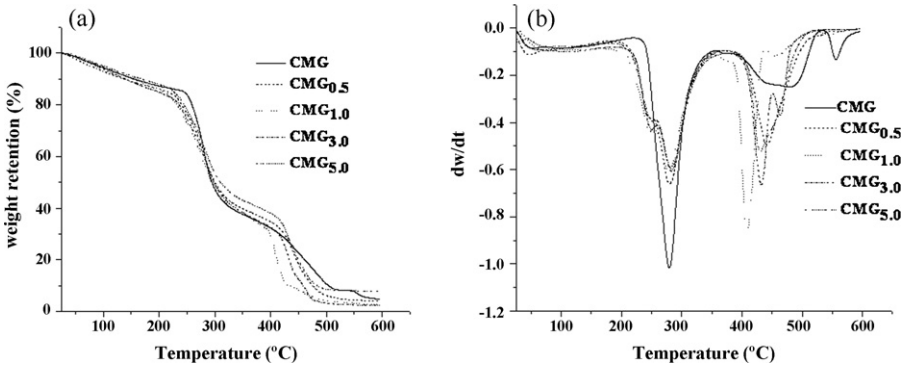

Fig. 3. (a) Thermogravimetry (TG) and (b) derivative thermogravimetry (DTG) plots of CMG and its hybrid nanocomposites under nitrogen.

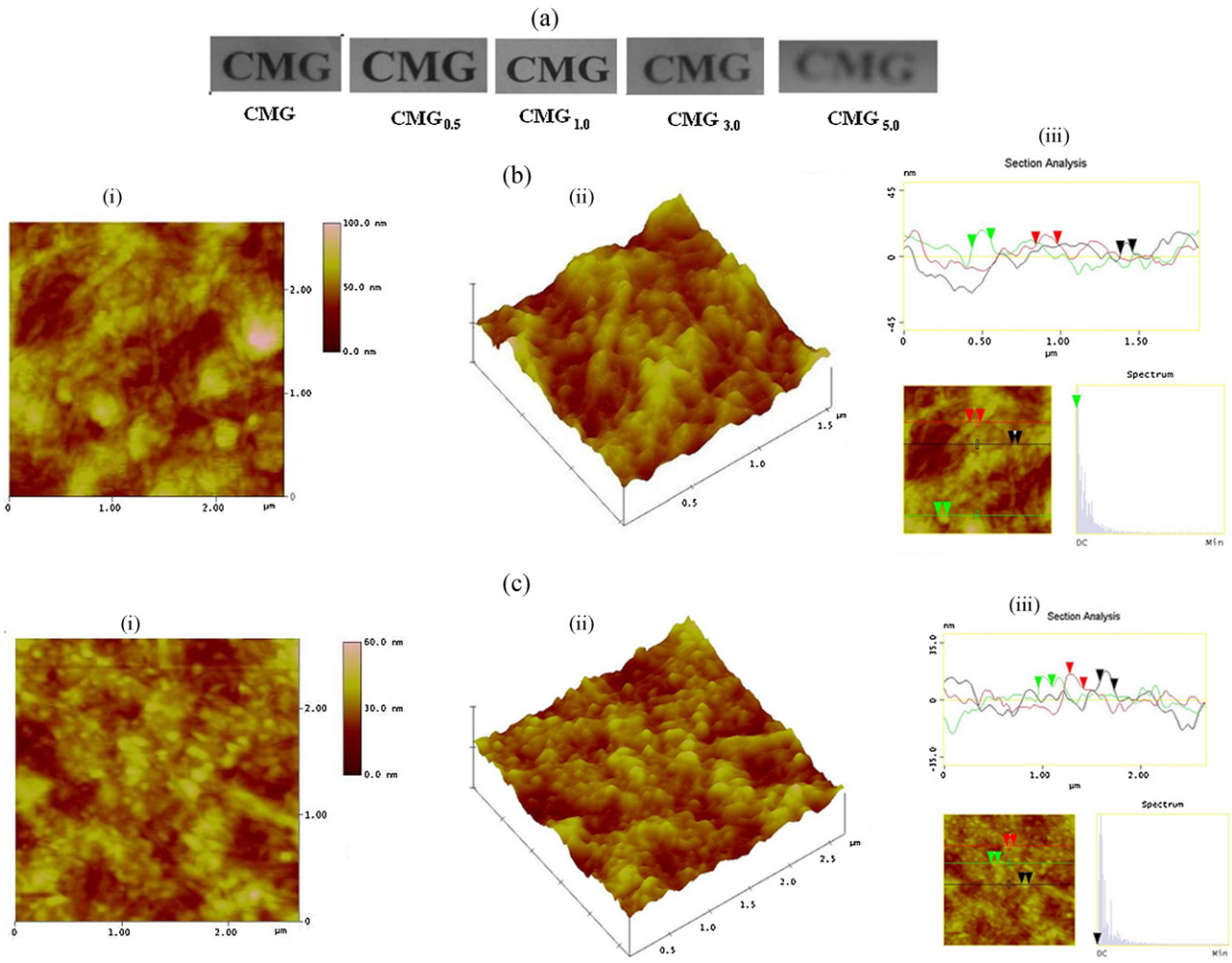

Fig. 4. (a) Photographic images of neat CMG and its hybrid nanocomposites and tapping mode Atomic Force Microscopic (b): (i) phase (ii) height and (iii) sectional images of $CMG_{0.5}$ and similar category of images of $CMG_{1.0}$ in (c): (i), (ii) and (iii), respectively.

insights. Topographic and phase contrast images of these samples are shown in Fig. 4b. The hard crystalline white domains observed in these phase images designate nanosilica and the gray portion indicates softer CMG matrix. In $CMG_{0.5}$ i.e. at low concentration, nanosilica particles predominantly orients into fine network structure of average line width 90 nm (section analysis image in Fig. 4b (iii)). These silica network bulge out of the matrix due to wide difference in surface energy with CMG (height image in Fig. 4b (ii)). In $CMG_{1.0}$ the silica network breaks into discrete silica nanoparticles with an average diameter of 120 nm (Fig. 4c (i)). It is produced from stronger CMG–silica interaction utilizing uncondensed surface silanol groups. We have already presumed this trend during ^{29}Si NMR analysis. The topographic image (Fig. 4c (ii)) shows lower peak to valley roughness (80 nm) as compared to $CMG_{0.5}$ (120 nm) which means better phase compatibility achieved between CMG and nanosilica at 1 wt% silica content. Visual appearance study excellently compliments morphological evidence. Neat CMG, $CMG_{0.5}$ and $CMG_{1.0}$ are visually transparent and appear identical. $CMG_{3.0}$ and $CMG_{5.0}$ are hazy due to scattering effect of the visual light from bigger silica aggregates.

3.5. Swelling analysis

Room temperature swelling behavior of neat CMG and its hydrogel nanocomposites have been studied till dissolution and the profiles are displayed in Fig. 5. Neat CMG shows extremely fast water intake capacity which drastically decreased in its nanocomposites. It swells extremely fast due to its highly polar mobile segments which makes way for the diffusing water molecules. Swelling is retarded due to generation of more restricted,

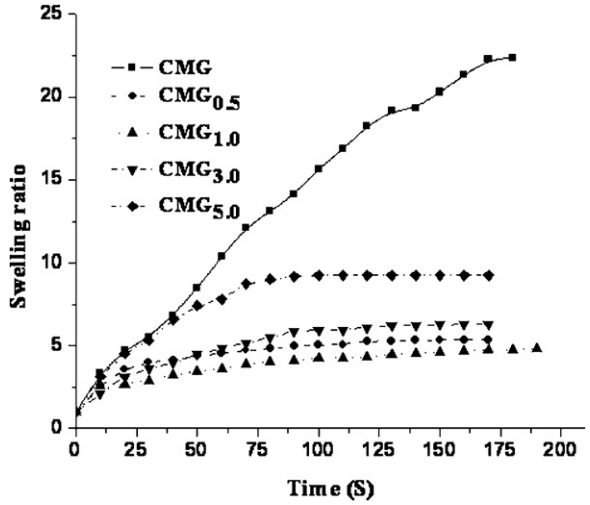

Fig. 5. Room temperature swelling kinetic study of neat CMG and its hybrid nanocomposites in dry state.

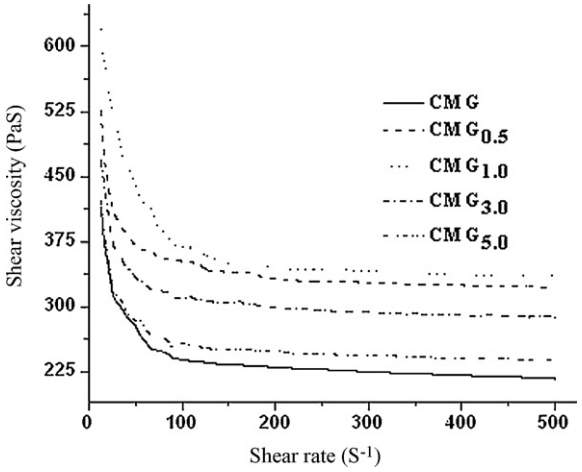

Fig. 6. Shear viscosity vs. shear rate plots of neat CMG and its hybrid nanocomposites.

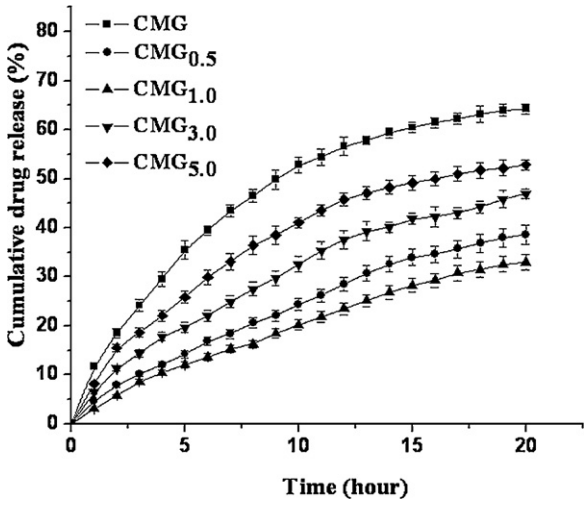

Fig. 7. Cumulative drug release (in percent) profiles of neat CMG and its hybrid nanocomposites. The results are mean ± SD ($n = 3$).

immobilized segments in its nanocomposites owing to adsorption over dispersed nanosilica particles. Swelling is minimum in $CMG_{1.0}$ followed by $CMG_{0.5}$, $CMG_{3.0}$, $CMG_{5.0}$, in increasing order. Since CMG has produced better organic–inorganic phase mixing using 1 wt% nanosilica, numerous immobilized CMG domains exists at this concentration making it most hydrophobic in character. At higher silica concentration, larger silica aggregates reduce adsorbate area and exposes more CMG segments for free or unperturbed swelling.

3.6. Rheological behavior analysis

Room temperature rheological behavior of neat CMG and its hybrid nanocomposites is compared in Fig. 6. All hydrogel nanocomposites including neat CMG are pseudoplastic. $CMG_{1.0}$ shows the highest initial viscosity followed by $CMG_{0.5}$, $CMG_{3.0}$, and $CMG_{5.0}$. Viscosity profile of neat CMG closely matches with that of $CMG_{5.0}$. At high shear rate regime $CMG_{5.0}$ shows distinctly low viscosity than rest of the nanocomposites. Since all the nanocomposites are hetero phase, rise in solution viscosity clearly implies CMG–nanosilica interaction generating more restrained CMG segments as presumed in the preceding section. Maximum shear viscosity exhibited both at low and high shear rate regime by $CMG_{1.0}$ proves strongest CMG–nanosilica interaction at this composition. But, the level of interaction is not so great in $CMG_{0.5}$ due to nanosilica forming separate network morphology while in $CMG_{3.0}$ and $CMG_{5.0}$, the reason being the formation of large aggregated silica domains. Another evidence is pseudoplasticity, 'n' calculated from double logarithmic plot, which follows similar trend (Table 1). Higher n values for $CMG_{3.0}$ and $CMG_{5.0}$ indicates faster dewetting under shear while low 'n' values of $CMG_{0.5}$ and $CMG_{1.0}$ elucidates slower CMG–nanosilica disengagements under similar condition.

3.7. In vitro release study of diclofenac sodium

The cumulative percent release of encapsulated diclofenac sodium was studied for continuous 20 h and the release profiles are compared in Fig. 7. Standard deviation against each release data are also displayed in the figure. Neat CMG exhibits weak bursting profile, whereby 35% of the encapsulated drug has been released within first 5 h at a faster rate, there after it tends to slow down and finally 65% of the drug was released till completion. This release profile has close proximity with the time profile generally observed in conventional drug therapy. On contrary, the elution profiles of $CMG_{0.5}$, $CMG_{1.0}$, $CMG_{3.0}$, are more slow and sustained barring $CMG_{5.0}$ which, though weaker than neat CMG, exhibits initial bursting character. Low standard deviation (±3) indicates realism of the data acquired during experimentation.

The elution profiles exhibited by '$CMG_{0.5}$, $CMG_{1.0}$ and $CMG_{3.0}$, corroborate their respective swelling and viscosity profiles. The drug–composite interaction along with high viscous resistance offered against selfdiffusion of diclofenac sodium has considerably reduced the elution rate especially in $CMG_{1.0}$. On contrary $CMG_{5.0}$ shows lowest matrix resistance and possibly weakest drug–matrix interaction. More hydrophobic nature of $CMG_{1.0}$ and $CMG_{0.5}$ also additionally helped in retaining the drug for longer period as compared to both $CMG_{3.0}$ and $CMG_{5.0}$. Kinetic investigation, excluding neat CMG, on hydrogel nanocomposites is reported in Table 1. Neat CMG is excluded since it has displayed prominent bursting profile which is utterly different from its hybrid nanocomposites. The release profile is fitted with standard zero order, 1st order, Higuichi and Korsmayer–Peppas kinetic models. Regression values up to five decimal places are calculated and it shows Korsmayer–Peppas model as the best fit model for all the hydrogels (Table 1). Eq. (1) shows the expression of this model:

$$\frac{M_t}{M\infty} = kt^m \tag{1}$$

M_t denotes drug concentration after time interval t and M_∞ is the equilibrium release concentration. K is a constant related to drug morphology which is constant for all the four nanocomposites. The release mechanism of drug molecules can be determined from the 'm' value. 'm' values for all the hydrogels are calculated from their logarithmic plot. All values are greater than 0.5 which indicates nonFickian release mechanism which is controlled by relative relaxation profiles of CMG segment. Better CMG–nanosilica adhesion in $CMG_{1.0}$ and $CMG_{0.5}$ generating more immobile CMG segments virtually leads to slower release compared to $CMG_{3.0}$ where such immobile domains are far less.

4. Conclusion

More uniform, nanoscale dispersion of silica in CMG has been achieved at lower concentration i.e. at 0.5 and 1 wt% than at higher concentration levels. High temperature stability of all the nanocomposites is poor but hybrids with low nanosilica contents are thermally more stable than neat CMG up to 270 °C mainly due to high hydrophobicity and CMG–silica adhesion (mechanical strength). These further advocated for their high solution viscosities both at low and high shear rate regimes. Rest of the hybrids

fails to meet the deserving balance between high hydrophobicity and mechanical strength. $CMG_{0.5}$ and $CMG_{1.0}$ produce slow and steady transdermal release following non-Fickian mechanism which results from their efficient drug encapsulation potential. Low matrix viscosity followed by high hydrophilicity of neat CMG and $CMG_{5.0}$ results into burst-assisted faster release profile. $CMG_{1.0}$ gives slowest release due to stringent balance between deserved properties and thus shows great promise towards future application.

Acknowledgement

The first author and the corresponding author both acknowledges financial help provided by Centre for Research in Nanoscience and Nanotechnology, University of Calcutta to carry out this project.

References

Adnadjevic, B., Jovanovic, J. & Drakulic, B. (2007). Isothermal kinetics of (E)-4-(4-metoxyphenyl)-4-oxo-2-butenoic acid release from a poly (acrylic acid) hydrogel. *Thermochimica Acta*, *466*, 38–48.

Ali, M., Horikawa, S., Venkatesh, S., Saha, J., Hong, J. W. & Byrne, M. E. (2007). Zero-order therapeutic release from imprinted hydrogel contact lenses within *in vitro* physiological ocular tear flow. *Journal of Controlled Release*, *124*, 154–162.

Altman, R. & Barkin, R. L. (2009). Topical therapy for osteoarthritis: clinical and pharmacologic perspectives. *Postgraduate Medicine*, *121*, 139–147.

Bandyopadhyay, A., De Sarkar, M. & Bhowmick, A. K. (2005a). Poly (vinyl alcohol)/silica hybrid nanocomposites by sol–gel technique: Synthesis and properties. *Journal Materials Science (USA)*, *40*, 5233–5241.

Bandyopadhyay, A., De Sarkar, M. & Bhowmick, A. K. (2005b). Polymer–filler interactions in sol–gel derived polymer/silica hybrid nanocomposites. *Journal of Polymer Science Part B: Polymer Physics*, *43*, 2399–2412.

Bandyopadhyay, A., De Sarkar, M. & Bhowmick, A. K. (2006). Structure–property relationship in sol–gel derived polymer/silica hybrid nanocomposites prepared at various pH. *Journal of Materials Science*, *41*, 5981–5993.

Banning, M. (2006). The use of topical diclofenac for pain in osteoarthritis of the knee: A review. *British Journal of Community Nursing*, *114*, 87–92.

Bhunia, T., Goswami, L., Chattopadhyay, D. & Bandyopadhyay, A. (2011). Sustained transdermal release of diltiazem hydrochloride through electronbeam irradiated different PVA hydrogel membranes. *Nuclear Instruments and Methods in Physics Research B*, *269*, 1822–1828.

Cassano, R., Trombino, S., Muzzalupo, R., Tavano, L. & Picci, N. (2009). A novel dextran hydrogel linking trans-ferulic acid for the stabilization and transdermal delivery of vitamin E. *European Journal of Pharmaceutics and Biopharmaceutics*, *72*, 232–238.

Diez-Pascual, A. M., Naffakh, M., González-Domínguez, J. M., Anson, A., Martinez-Rubi, Y., Martinez, M. T., et al. (2010). High performance PEEK/carbon nanotube composites compatibilized with polysulfones-II. Mechanical and electrical properties. *Carbon*, *48*, 3500–3511.

Giri, A., Bhowmick, M., Pal, S. & Bandyopadhyay, A. (2011). Polymer hydrogel from carboxymethyl guar gum and carbon nanotube for sustained trans-dermal release of diclofenac sodium. *International Journal of Biological Macromolecules*, doi:10.1016/j.ijbiomac.2011.08.003

He, H., Cao, X. & Lee, L. J. (2004). Design of a novel hydrogel-based intelligent system for controlled drug release. *Journal of Controlled Release*, *95*, 391–402.

Ji, Q. X., Deng, J., Xing, X. M., Yuan, C. Q., Yu, X. B., Xu, Q. C., et al. (2010). Biocompatibility of a chitosan-based injectable thermosensitive hydrogel and its effects on dog periodontal tissue regeneration. *Carbohydrate Polymers*, *82*, 1153–1160.

Lee, C. T., Kung, P. H. & Lee, Y. D. (2005). Preparation of poly (vinyl alcohol)–chondroitin sulfate hydrogel as matrices in tissue engineering. *Carbohydrate Polymer*, *61*, 348–354.

Liang, S., Xu, J., Weng, L., Dai, H., Zhang, X. & Zhang, L. (2006). Protein diffusion in agarose hydrogel in situ measured by improved refractive index method. *Journal of Controlled Release*, *115*, 189–196.

Lin, Y., Chen, Q. & Luo, H. (2007). Preparation and characterization of N-(2-carboxybenzyl)chitosan as a potential pH-sensitive hydrogel for drug delivery. *Carbohydrate Research*, *342*, 87–95.

Lolis, M., Toosi, S., Czernik, A. & Bystryn, J. C. (2011). Effect of intravenous immunoglobulin with or without cytotoxic drug on pemphigus intercellular antibodies. *Journal of the American Academy of Dermatology*, *64*, 484–489.

Magnette, J., Kienzler, J. L., Alekxandrova, I., Savaluny, E., Khemis, A., Amal, S., et al. (2004). The efficacy and safety of low-dose diclofenac sodium 0.1% gel for the symptomatic relief of pain and erythema associated with superficial natural sunburn. *European Journal of Dermatology*, *14*, 238–246.

Meenach, S. A., Hilt, J. & Anderson, Z. K. W. (2010). Poly (ethylene glycol)-based magnetic hydrogel nanocomposites for hyperthermia cancer therapy. *Acta Biomaterialia*, (6), 1039–1046.

Moskowitz, J. S., Blaisse, M. R., Samuel, R. E., Hsu, H. P., Harris, M. B., Martin, S. D., et al. (2010). The effectiveness of the controlled release of gentamicin from polyelectrolyte multilayers in the treatment of *Staphylococcus aureus* infection in a rabbit bone model. *Biomaterials*, *31*, 6019–6030.

Nugent, M. J. D. & Higginbotham, C. L. (2007). Preparation of a novel freeze thawed poly (vinyl alcohol) composite hydrogel for drug delivery applications. *European Journal of Pharmaceutics and Biopharmaceutics*, *67*, 377–386.

Pal, S. (2009). Carboxymethyl guar: Its synthesis and macromolecular characterization. *Journal of Applied Polymer Science*, *111*, 2630–2636.

Peng, K. T., Chen, C. F., Chu, I. M., Li, Y. M., Hsu, W. H., Hsu, R. W. W., et al. (2010). Treatment of osteomyelitis with teicoplanin-encapsulated biodegradable thermosensitive hydrogel nanoparticles. *Biomaterials*, *31*, 5227–5236.

Siddaramaiah, Kumar, P., Divya, K. H., Mhemavathi, B. T. & Manjula, D. S. (2006). Chitosan/HPMC polymer blends for developing transdermal drug delivery systems. *Journal of Macromolecular Science, Part A: Pure and Applied Chemistry*, *43*, 601–607.

Singh, B. & Pal, L. (2008). Development of sterculia gum based wound dressings for use in drug delivery. *European Polymer Journal*, *44*, 3222–3230.

Spitalsky, Z., Tasis, D., Papagelis, K. & Galiotis, C. (2010). Carbon nanotube–polymer composites: Chemistry, processing, mechanical and electrical properties. *Progress in Polymer Science*, *35*, 357–401.

Srinivas, P., Sunitha, M., Babu, D. S. R. & Sadanandam, M. (2011). Preparation and evaluation of colon-specific controlled release capecitabine matrix tablets using a novel drug carrier. *International Journal of Pharmaceutical Science*, *3*, 1152–1162.

Trachsel, D., Tschudi, P., Portier, C. J., Kuhn, M., Thormann, W., Scholtysik, G., et al. (2004). Pharmacokinetics and pharmacodynamic effects of amiodarone in plasma of ponies after single intravenous administration. *Toxicology and Applied Pharmacology*, *195*, 113–125.

Tjong, S. C. (2006). Structural and mechanical properties of polymer nanocomposites. *Materials Science and Engineering*, *53*, 73–197.